

First-Principles Theory, Coarse-Grained Models, and Simulations of Ferroelectrics

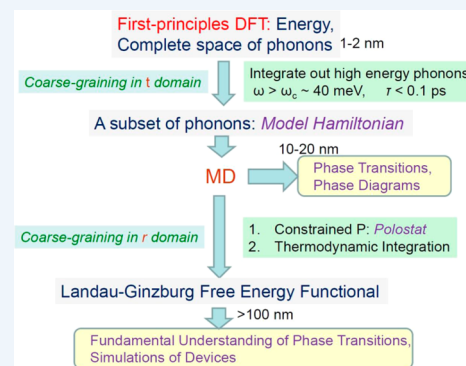
Umesh V. Waghmare*

Theoretical Sciences Unit and Sheikh Saqr Laboratory, J Nehru Centre for Advanced Scientific Research, Jakkur PO, Bangalore 560 064 India

CONSPECTUS: A ferroelectric crystal exhibits macroscopic electric dipole or polarization arising from spontaneous ordering of its atomic-scale dipoles that breaks inversion symmetry. Changes in applied pressure or electric field generate changes in electric polarization in a ferroelectric, defining its piezoelectric and dielectric properties, respectively, which make it useful as an electromechanical sensor and actuator in a number of applications. In addition, a characteristic of a ferroelectric is the presence of domains or states with different symmetry equivalent orientations of spontaneous polarization that are switchable with large enough applied electric field, a nonlinear property that makes it useful for applications in nonvolatile memory devices. Central to these properties of a ferroelectric are the phase transitions it undergoes as a function of temperature that involve lowering of the symmetry of its high temperature centrosymmetric paraelectric phase.

Ferroelectricity arises from a delicate balance between short and long-range interatomic interactions, and hence the resulting properties are quite sensitive to chemistry, strains, and electric charges associated with its interface with substrate and electrodes. First-principles density functional theoretical (DFT) calculations have been very effective in capturing this and predicting material and environment specific properties of ferroelectrics, leading to fundamental insights into origins of ferroelectricity in oxides and chalcogenides uncovering a precise picture of electronic hybridization, topology, and mechanisms. However, use of DFT in molecular dynamics for detailed prediction of ferroelectric phase transitions and associated temperature dependent properties has been limited due to large length and time scales of the processes involved. To this end, it is quite appealing to start with input from DFT calculations and construct material-specific models that are realistic yet simple for use in large-scale simulations while capturing the relevant microscopic interactions quantitatively.

In this Account, we first summarize the insights obtained into chemical mechanisms of ferroelectricity using first-principles DFT calculations. We then discuss the principles of construction of first-principles model Hamiltonians for ferroelectric phase transitions in perovskite oxides, which involve coarse-graining in time domain by integrating out high frequency phonons. Molecular dynamics simulations of the resulting model are shown to give quantitative predictions of material-specific ferroelectric transition behavior in bulk as well as nanoscale ferroelectric structures. A free energy landscape obtained through coarse-graining in real-space provides deeper understanding of ferroelectric transitions, domains, and states with inhomogeneous order and points out the key role of microscopic coupling between phonons and strain. We conclude with a discussion of the multiscale modeling strategy elucidated here and its application to other materials such as shape memory alloys.



INTRODUCTION

A piezoelectric material is a dielectric insulator in which macroscopic electric dipole (polarization) is induced along with a mechanical deformation in response to external pressure or stress. This polarization is a result of noncentrosymmetric rearrangement of its electronic charge and polar bonds, and hence a piezoelectric crystal necessarily lacks inversion symmetry. Ferroelectrics form a subclass of piezoelectric materials,¹ which possess an electrically switchable macroscopic polarization spontaneously, that is, even in the absence of applied electric or stress fields. Moreover, this spontaneous polarization vanishes above a Curie temperature as the ferroelectric crystal transforms to a higher symmetry, centrosymmetric paraelectric phase. The inversion symmetry of the parent paraelectric phase implies at least two orientations

of the spontaneous polarization (P and $-P$) of the ferroelectric phase, and switching between them is possible with large enough electric field. Such nonlinear switching response of a ferroelectric is relevant to its use as a memory device, while its linear piezoelectric response is crucial to its large number of technological applications in micro-electromechanical systems.

Mechanisms of linear and nonlinear responses of a ferroelectric involve many low symmetry states that result from breaking of different symmetries of the paraelectric phase, which are readily accessible as fluctuations of the equilibrium

Special Issue: DFT Elucidation of Materials Properties

Received: September 7, 2014

Published: October 31, 2014

state near the ferroelectric phase transition at Curie temperature. As a result, piezoelectric and dielectric responses are anomalously large and electric fields for switching response are small near the transition. This is the reason the most commonly used ferroelectric involves a composition $x \approx 0.52$ of $\text{PbZr}_{1-x}\text{Ti}_x\text{O}_3$ (PZT), at which the material is close to a structural transition from tetragonal to rhombohedral ferroelectric state at all temperatures (see Figure 1a). Indeed, it is

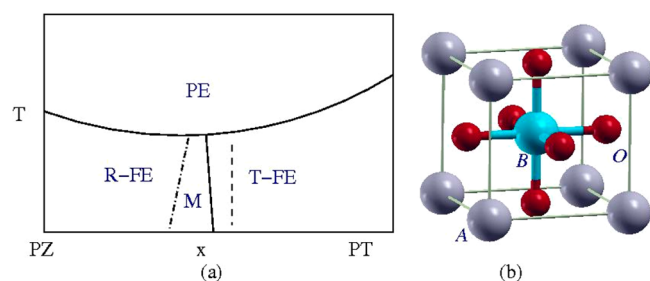


Figure 1. (a) A sketch of a phase diagram of $\text{PbZr}_{1-x}\text{Ti}_x\text{O}_3$ (PZT), with rhombohedral and tetragonal phases separated by a morphotropic phase boundary (a solid line) and M indicates the presence of monoclinic and other phases. Dashed line indicates the useful composition at which PZT is always close to a transition. (b) ABO_3 compound in the cubic perovskite structure.

essential to develop fundamental understanding of chemistry and physics of ferroelectric phase transitions to be able to design novel and high performance ferroelectrics.

Most technologically important ferroelectrics are ABO_3 perovskite oxides (see Figure 1b) involving a 3d transition metal (TM) at the B site. First-principles density functional theoretical techniques are ideally suitable to capture the relative energetics of paraelectric and various low symmetry structures of such a ferroelectric, particularly because electron correlations do not have significant effect on properties of room or high temperature ferroelectrics. An initial major breakthrough was based on all electron DFT calculations,² which revealed the crucial role of the hybridization between 3d states of TM and 2p states of oxygen in giving rise to ferroelectricity in perovskite oxides. The development of cost-effective and accurate pseudopotentials^{3,4} triggered the widespread use of first-principles DFT calculations in understanding the structure and chemistry dependent properties of ferroelectrics.⁵ It was further enhanced with the availability of DFT-linear response techniques.^{6,7}

Interestingly, polarization of a periodic crystal cannot be determined from charge density alone, and fundamental studies of ferroelectrics fueled advances in DFT techniques as well: Berry phase theory of polarization⁸ and real-space partitioning of charge density of a periodic structure using maximally localized Wannier functions.⁹ While the former is relevant to electronic properties of topological insulators, the latter is commonly used in a variety of problems tackled by DFT. Along with the atomic scale control on the structure of interfaces and films of oxide materials that is now possible experimentally,¹⁰ these advances have led over the last 20 years to paradigmatic shift in understanding of ferroelectric materials,^{11,12} and even prediction of novel ferroelectrics like BiAlO_3 entirely from first-principles.¹³

Though DFT techniques are quite effective in estimating the energetics of structures relevant to ferroelectric phase transitions, they are still computationally too expensive to be

used directly in statistical mechanical analysis of the transition or capturing the properties of inhomogeneously ordered states like ferroelectric domains, which are key to phase transitions and performance of nanoscale devices. These occur on the length scales of several nanometers and time scales that vary from 10s of picoseconds to microseconds and require simulations of several thousand configurations of hundreds of atoms, which are presently impractical due to computational intensity. A multiscale modeling strategy is thus necessary to expand the reach of DFT techniques to a wider range of phenomena in ferroelectrics, while developing their deeper understanding.

In this Account, we highlight the insights into chemistry and microscopic physics that govern the technologically important properties of ferroelectrics, as determined using first-principles DFT calculations and multiscale modeling. This is essentially based on our own work and not intended to be a review covering the vast literature based on the works of several groups. We first present the precise chemical mechanisms with quantitative estimates of their contributions to a property that signifies the tendency of a material to turn ferroelectric. We summarize the principles of coarse-graining in time domain to construct a lattice model of a ferroelectric and illustrate its applications through MD simulations to determine phase diagrams of bulk and nanoscale ferroelectric films. We then present a method for coarse-graining in real space that uses MD to determine the free energy landscape of a ferroelectric as a function of spatially varying polarization and temperature. This provides a simple framework to understand behavior of a ferroelectric subject to various boundary conditions in bulk as well as at nanoscale. We point out the importance of spatial fluctuations in polarization to phase transition behavior and related properties of a ferroelectric and identify the microscopic coupling between strain and polar phonon as the fundamental interaction that controls them.

CHEMICAL MECHANISMS OF FERROELECTRICITY

While ferroelectricity may arise from the broken inversion symmetry of the electronic structure, the relevant energy scales are small, and it occurs at low temperatures. As reported recently, the simplest material to exhibit ferroelectricity is trigonal Se, in which ferroelectricity arises from symmetry lowering ordering of the spins of electronic states localized at the surface,¹⁴ as a consequence of electronic topology and chiral structure. Ferroelectricity in ABO_3 perovskites (see Figure 1b) is primarily structural in origin involving a polar optic phonon. For example, macroscopic polarization in BaTiO_3 arises from off-center displacement of Ti with respect to its centrosymmetric position at the center of TiO_6 octahedron. In contrast, BaZrO_3 does not exhibit any ferroelectricity, and such differences can be understood only in terms of electronic structure and the nature of chemical bonding and mechanisms.

In an insulator, Born dynamical charge (Z^*) of an atom is often a good indicator of its tendency to displace off-center and give rise to electric dipole moment.^{15,16} The charge gives a force $F = Z^*E$ felt by an atom as a result of electric field E or the dipole moment $p = Z^*u$ induced by its displacement u . Deviation of Z^* with respect to the nominal ionic charge quantifies the charge anomaly and ion's ability to spontaneously displace off-center and contribute to ferroelectricity. For example, Z^* of Ti and Zr in BaTiO_3 and BaZrO_3 are 7.2 and 5.7, respectively.^{15,17} While the p-d hybridization has been

shown to be relevant to anomalous dynamical charges,^{18,19} the precise mechanism of charge transfer¹⁹ can be explicitly and quantitatively analyzed shown by real-space partitioning and connecting with atomic orbitals. To this end, projection of Wannier functions²⁰ on d orbitals of TM and p orbitals of O was used to quantify contributions of covalency, local polarizability, and charge transfer to Z^* .¹⁷ While the contributions of covalency and polarizability of oxygen to Z^* of Ti are $1.2e$ and $-0.15e$, respectively, and those to Z^* of Zr are $1.6e$ and $-0.3e$, it was the *long-range* charge transfer that was a clear distinguishing mechanism: it contributed $2.9e$ and $1.6e$, respectively to Z^* of Ti and Zr. This charge transfer involves hopping of a tiny electronic charge from the d orbital of one TM to that of another via p orbitals of the bridging O, in the direction opposite to the displacement of the TM (see Figure 2) and is analogous to the double exchange mechanism in

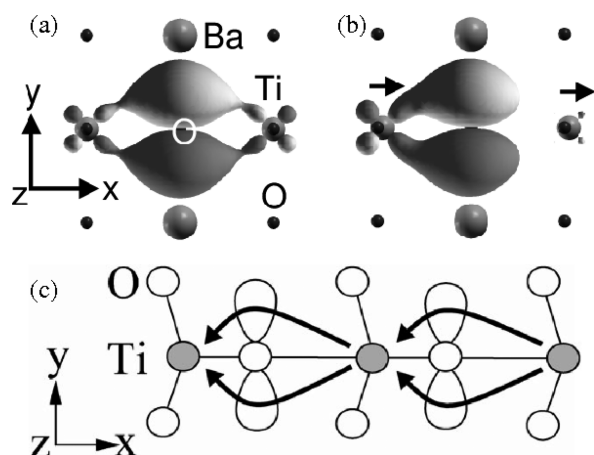


Figure 2. Wannier function with the character of a p_y orbital of oxygen (a) in the centrosymmetric state and (b) in the state with Ti displaced to the right (in BaTiO_3) and (c) a sketch showing accompanying electronic charge transferred from one Ti to the next by hopping via the p orbital of the bridging oxygen. Analogous to the double exchange mechanism, this long-range charge transfer is the dominant chemical mechanism contributing to Born dynamical charge of Ti and its contribution to ferroelectricity (taken from ref 17).

magnetic oxides. Because the mechanism of charge transfer is expected to be sensitive to strain and stronger for smaller Zr–O bonds, unstable polar modes²¹ are indeed expected for SrZrO_3 , which has a smaller lattice constant than BrZrO_3 .

We close this section by pointing out that the Born charge of Se in trigonal crystal of Se is 0.70 ,¹⁴ while one naively expects ionic charges in a mono-elemental solid to be zero! The non-zero Born charge of Se itself is anomalous and results from its chiral structure, giving a clue to its unusual ferroic properties. Second, the stereochemical activity¹⁶ of the lone pair of 6s electrons of Pb^{2+} and Bi^{3+} is known to be relevant to ferroelectricity in Pb-based perovskites, and is also reflected in the anomalous Born charge of Pb ($Z^* = 3.90$). Such chemical considerations and first-principles calculations led to prediction of a novel high temperature ferroelectric,¹³ BiAlO_3 , which was later verified experimentally. While anomalous charges are generally good indicators of ferroelectricity, we note that not all ferroelectrics, particularly the improper or nonionic types, exhibit anomalous Born charges.²²

■ LATTICE MODEL OF A FERROELECTRIC: COARSE-GRAINING IN TIME DOMAIN

We now illustrate a strategy for construction of a model for ferroelectric transitions in a perovskite oxide. For statistical thermodynamic analysis of the ferroelectric or structural transition, one needs the energy of a material as a function of atomic positions. Since the low energy structures in the phase space relevant to ferroelectric transition can be obtained as distortions of the high-symmetry paraelectric phase, it is convenient to think of the energy function as a Taylor expansion in atomic displacements with respect to the paraelectric (cubic perovskite) structure. With first-order terms vanishing due to symmetry, quadratic terms are the lowest order terms that describe energetics of vibrations or phonons within harmonic approximation and are readily obtained from DFT linear response calculations.^{6,7}

Because the cubic structure of a ferroelectric perovskite is unstable at $T = 0$ K, many of the frequencies in its vibrational spectrum determined within DFT are imaginary ($\omega^2 < 0$), meaning that a cubic structure is *NOT* a local minimum of energy function. These constitute the unstable modes or lattice

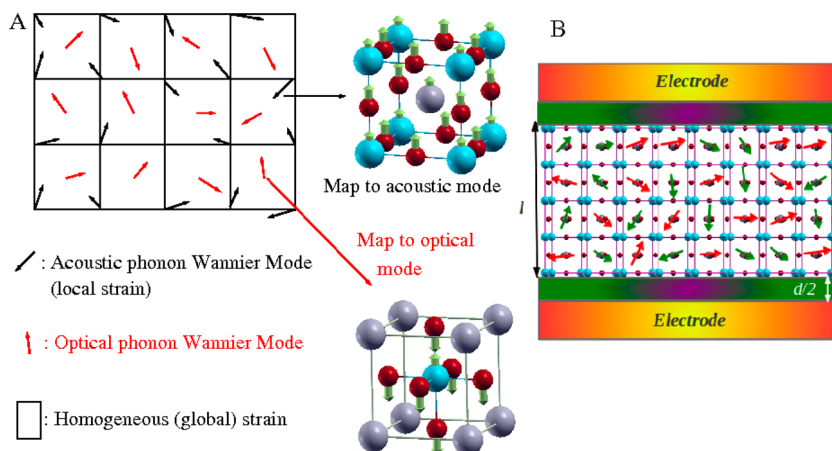


Figure 3. Lattice model of BaTiO_3 with u_i 's and η_i 's representing Ti- and Ba-centered phonon Wannier vector modes localized in the i th unit cell, which map to atomic displacements that constitute unstable optic and acoustic phonons, respectively. On the right, electrodes are shown as perfect electrostatic mirrors separated from the ferroelectric film by a vacuum of thickness $d/2$ (arrows denote u_i Wannier modes). Panel B is taken from ref 39.

instabilities of the material, and the eigenvector of the strongest instability gives the relative displacements of atoms that are relevant to the phase transition. Typically, a cubic perovskite exhibits two sets of competing instabilities:²³ polar ones involving cation displacement off-center and nonpolar ones involving TMO₆ octahedral rotations. While the former give rise to ferroelectricity, the latter participate in antiferrodistortive or antiferroelectric phase transitions. The first step in construction of a model is to identify the symmetry invariant subspace (bands) of phonons that contain the dominant instabilities.

In the second step, one notes that high frequency phonons couple with the unstable phonons only at higher (>2) order and verifies an assumption that their coupling is weak. As a result, these modes ($\nu > 10$ THz) are integrated out analytically from the partition function with a trivial contribution to free energy. In the third step, one uses the phonon Wannier modes²⁴ as a localized basis to span and project into the subspace containing unstable modes. For example, Ti-centered three-dimensional Wannier vector modes (\mathbf{u}_i 's, localized in the i th unit cell) map to subspace of unstable polar optical phonons, and Ba-centered 3-D Wannier vector modes ($\boldsymbol{\eta}_i$'s) map to the entire subspace of acoustic phonons. Thus, the model consists of a pair of 3-D vectors (\mathbf{u}_i 's and $\boldsymbol{\eta}_i$'s) in each unit cell and six components of the homogeneous strain tensor (see Figure 3A). The subspace of phonons containing competing unstable modes involving TMO₆ octahedral rotations needs to be included to model a material like SrTiO₃, which exhibits a transition to an antiferrodistortive phase.²⁵ In the fourth step, the model Hamiltonian H is expanded as a Taylor series in strain, \mathbf{u}_i 's and $\boldsymbol{\eta}_i$'s, such that it is invariant under the symmetries of the paraelectric cubic structure.

The quadratic terms in the model energy H capture the interatomic spring or force constants relevant to the unstable optic and acoustic modes,^{26,27} higher order terms in \mathbf{u}_i 's to capture the anharmonic interactions necessary for the thermal stability of cubic phase at high temperatures; elastic energy associated with strain and the third order coupling of \mathbf{u}_i 's with strain and $\boldsymbol{\eta}_i$'s: the strain-phonon coupling. We note that the harmonic interactions include long-range dipolar interaction between \mathbf{u}_i 's, which is often a bottleneck in large scale MD or MC simulations. These, along with the coupling between \mathbf{u}_i 's and $\boldsymbol{\eta}_i$'s, can be tackled efficiently in reciprocal space by employing FFT algorithm: long-range interactions in real-space are local in reciprocal space.²⁸ An open-source code²⁹ (FERAM) based on this algorithm³⁰ can be used readily for mixed-space molecular dynamics of H to simulate systems at fairly large scales (~20 nm and 10s of nanoseconds) on moderate computing resources.

Bulk Ferroelectrics

Use of model Hamiltonians of BaTiO₃²⁶ and PbTiO₃²⁷ in FERAM based MD simulations reproduces³¹ (a) the observed sequence of three phase transitions from cubic to tetragonal (C–T), tetragonal to orthorhombic, and orthorhombic to rhombohedral ferroelectric phases of BaTiO₃ and the contrasting single C–T phase transition in PbTiO₃ and (b) the first-order character of these transitions, with underestimated T_c 's within 100 K of the experimental T_c 's. A systematic analysis³² of the estimation of T_c 's from first-principles showed that much of the error comes from the underestimation of lattice constants in DFT with a local density

approximation of exchange correlation energy. Improved functional by Wu and Cohen gives better estimation of T_c 's, but it significantly improves the accuracy if one includes negative pressure to match the lattice constant with experiment as a function of T .³²

Electric field can be readily included in H by adding a term $-ZE\sum_{i=1}^N(\mathbf{u}_i)$, where Z is the mode effective charge of the unstable optic phonon. With use of this in FERAM simulations, electric phase–temperature phase diagrams were determined³³ of bulk BaTiO₃, which revealed the regions of stability of monoclinic phases in the E – T plane (see Figure 4), which were

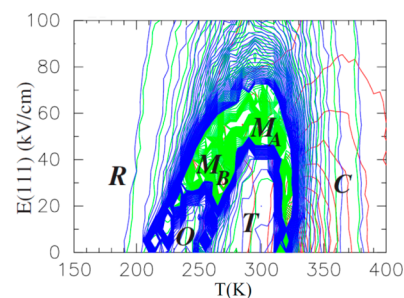


Figure 4. Electric field (along (111) direction)–temperature phase diagram of BaTiO₃, expressed as a contour-plot of dielectric response determined from FERAM simulations, revealing the presence of different monoclinic phases that are relevant to giant electro-mechanical response (taken from ref 33).

shown in DFT calculations to be the transition states during polarization rotation, the mechanism responsible for the giant electromechanical response of perovskite ferroelectrics.³⁴ Indeed, such MD simulations can also be used to determine the nonlinear polarization response of a ferroelectric to applied electric field (hysteresis).³⁵ Such simulations yield rather large overestimation coercive field, the field required to reverse the direction of polarization. This is because the simulations are unable to span the length scales and time scales relevant to nucleation of ferroelectric domains,³⁶ pointing to the need for further multiscale modeling.

Nanoscale Ferroelectrics: FERAM Simulations

Effects of electrodes on ferroelectricity in nanoscale films of BaTiO₃ have been studied using first-principles calculations,³⁷ but such analysis can access phenomena only at very small length scales. Simulations with model Hamiltonian with inclusion of a simple term with depolarization field³⁸ was shown to result in inhomogeneous ordering with formation of domains. As shown in Figure 3B, a thin film of a model ferroelectric sandwiched between more realistic electrodes can be simulated with FERAM code. When the thickness of vacuum $d = 0$, electrodes are perfect in screening the surface charges of the film, and the resulting depolarization field vanishes. If $d = 1$ unit cell, the electrodes are imperfect and only partially screen the surface charges, with a nonzero depolarization field. By imposing mechanical boundary conditions with fixed in-plane lattice constants of a film, one can simulate epitaxial films with a given epitaxial strain. The nature of electrodes has remarkable consequences to ferroelectric transitions: when epitaxial strain is compressive, one gets a bulk-like tetragonal ferroelectric phase when they are perfect, while a striped phase with 180° domains appears below Curie temperature when the electrodes are imperfect.³⁹ While the transition temperature in the latter is lower due to the depolarizing field, the transition temperatures

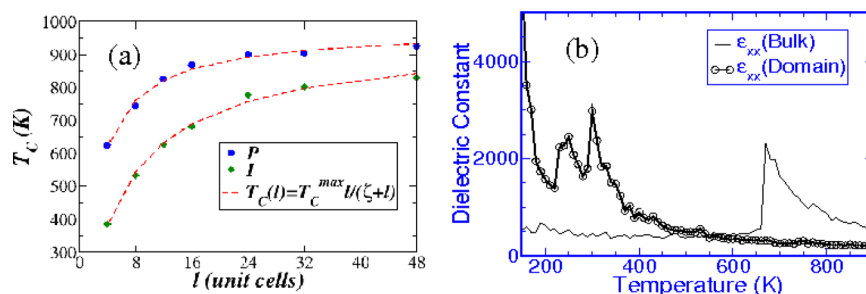


Figure 5. Size dependence of the temperature of ferroelectric transition in epitaxial films of PbTiO_3 sandwiched between perfect (P) and imperfect (I) electrodes (a) (taken from ref 39), and giant dielectric response of PbTiO_3 with 180° domains in comparison with that of bulk (b) (taken from ref 40).

are enhanced relative to its bulk value due to epitaxial strain (see Figure 5a). They increase with thickness and saturate beyond the thickness of 12 nm.

Epitaxial strain–temperature phase diagrams determined using FERAM simulations of BaTiO_3 films³¹ show tunability of ferroelectric transition temperatures with strain and a crossover from a stable tetragonal FE phase in films with compressive strain to a stable orthorhombic FE phase in films with tensile strains when the electrodes are perfect. In contrast, the strain–temperature phase diagram of PbTiO_3 films with imperfect electrodes reveals the possibility of strain engineering of the domain structure in ultrathin films³⁹ (see Figure 6). At

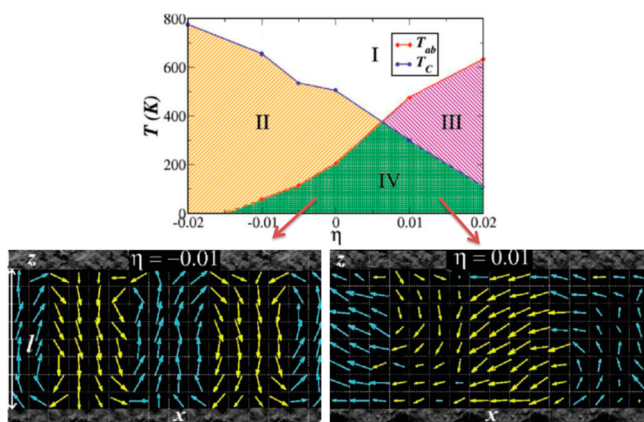


Figure 6. Phase diagram and strain engineering of the inhomogeneously ordered ferroelectric states and domain structure in epitaxial films of PbTiO_3 sandwiched between imperfect electrodes (taken from ref 39).

large compressive strain, 180° domain structure is more stable in the film. For intermediate compressive strains, the film exhibits a flux closure striped phase and rectangular wave-like 90° domains, while maintaining the in-plane 90° domain structure.

While MD simulations with a model ferroelectric using FERAM have been quite effective in the determination of phase transitions and phase diagrams of bulk and ultrathin epitaxial films, they are limited in capturing the processes at longer length and times scales that are involved in nucleation of domains and nonlinear switching response of polarization with electric field. Moreover, many ferroelectric oxides exhibit dielectric response with nontrivial dispersion at frequencies below 1 GHz, which is also presently beyond the reach of such MD simulations. Further coarse-graining to model phenomena at longer length scale is thus desirable.

FREE ENERGY LANDSCAPE OF FERROELECTRICS: COARSE-GRAINING IN REAL-SPACE

While estimation of absolute free energies (F) in MD simulations is quite hard, derivatives of free energy or differences in F involve calculation of thermodynamic averages and are readily determined in an MD simulation. Motivated by Landau theory, we set out to determine free energy as a function of polarization and temperature, relative to the free energy of the paraelectric state. Because polarization is an equilibrium property of a ferroelectric at a given T , access to free energy of a state with arbitrary polarization requires a “polostat”. This polostat can be physically interpreted as a fluctuating electric field that forces average polarization to a given value.⁴¹ The difference in free energies of the states with distinct values of polarization at a given T is obtained using thermodynamic integration and can be shown as the work done by the polostat field: $\Delta F = -\int_{P_1}^{P_2} E dP$.

By this approach, the free energy landscape of the cubic to tetragonal ferroelectric phase transition of BaTiO_3 reveals (see Figure 7) that the first-order character of the transition arises from a negative coefficient C_4 of the fourth order term: $\Delta F = C_2 P^2 + C_4 P^4 + C_6 P^6$. Physically it gives a free energy minimum at nonzero P corresponding to metastable ferroelectric phase

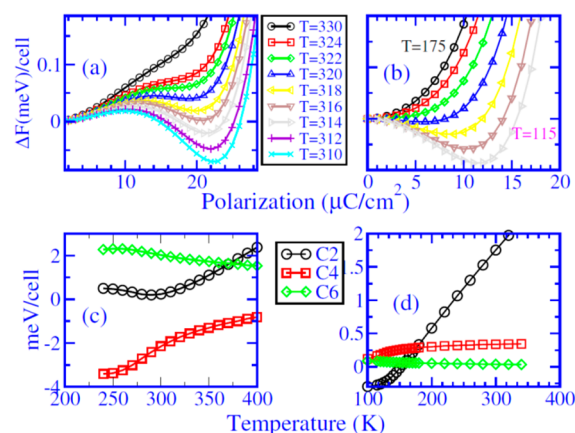


Figure 7. Polarization dependent free energy of the cubic to tetragonal phase transition of BaTiO_3 with (a) and without (b) inclusion of the strain–phonon coupling term in the model H_i , and temperature dependence of the associated coefficients of the second, fourth, and sixth order terms of free energy as a function of polarization in panels c and d. The negative coefficient C_4 (in panel c) is responsible for the first-order transition in panel a, while the second order transition in panel b is essentially controlled by the second order coefficient in panel d.⁴¹

just above the transition. At the microscopic level, it was shown³⁴ that the C–T transition becomes second order if the term with coupling between polar phonon and strain is omitted from the model H (see Figure 7). The free energy function of this transition follows the standard Landau like functional in which the second order coefficient C_2 is $A(T - T_c)$, see Figure 7. The fact that the second order coefficient C_2 remains positive (Figure 7a) even below the transition temperature is striking because it suggests metastability of the $P = 0$ state. A detailed examination of the dipolar field in the $P = 0$ state below $T = T_c$ reveals a spatially fluctuating polarization field. Thus, suppression of uniform polarization by any means leads to an equilibrium state with inhomogeneous ordering of dipoles, such as domain structure. This does not happen when the strain phonon coupling is turned off! Thus, the domain structure or polarization fluctuations are crucial to the first-order ferroelectric phase transitions, and they are controlled by the strain–phonon coupling at the microscopic level.⁴² This work⁴¹ has led to augmentation of the conventional Landau free energy functional with terms to include its dependence on divergence, curl, and other derivatives of polarization. Variational principle of the free energy results in a guideline that polarization field should be as divergence-free as possible.

Coarse-graining of short wavelength fluctuations in P through MD allows estimation free energies of domain walls as a function of T (see Figure 8). We find that 90° ferroelectric

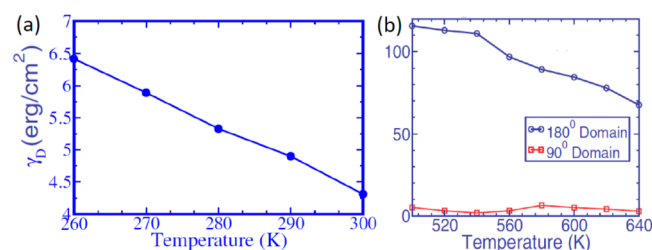


Figure 8. Domain wall energy for (a) 180° domains in BaTiO₃ and (b) 180° and 90° domains in PbTiO₃. We note that 90° domains are *not* stable in BaTiO₃.^{41,42}

domain walls are *not* stable in BaTiO₃, while they are an order of magnitude lower in energy than the 180° domain walls in PbTiO₃, and their free energy is comparable to that of 180° domain walls³⁴ in BaTiO₃. The specific details of such domain structure have also been shown to depend on the microscopic strain–phonon coupling⁴² in the model H . It is remarkable that these two steps of coarse-graining still preserve the material-specific properties. Before closing, such inhomogeneous ordering can significantly alter the properties of a ferroelectric. For example, a giant dielectric response⁴⁰ arises [see Figure 5b] of a configuration that is forced to have 180° domain structure in PbTiO₃.

■ RELATED PROBLEMS

Heterovalent cation substitution⁴³ in ferroelectric oxides often results in relaxor properties characterized by a glassy dielectric response with frequency dispersion obeying Vogel–Fulcher law. First-principles modeling and MD simulations have been used in addressing this problem that involves rather long length and time scales but with very limited success: mainly the correlation between a nanopolar region with chemically ordered substitution and a diffuse dielectric response has been established.⁴⁴ However, realistic treatment of the random

local electric fields, their dependence on nanoscale structure, and effects on sub-gigahertz dielectric properties remain to be understood. More recently, heterovalent anion substitution (N and F substitution for O) has been shown to result in diffuse dielectric response as well.⁴⁵ Similarly, atomically engineered superlattices and heterostructures¹⁰ can be interesting systems for fundamental understanding of novel phenomena in oxide ferroelectrics. Magnetically induced ferroelectrics exhibit large a magnetoelectric coupling and are quite interesting too but involve smaller energy scales and lower temperatures of ordering, where electron correlation effects can be important and challenging to be treated. Finally, hybrid structures obtained with a combination of ferroelectrics and other nanoscale materials like MoS₂ or polymers provide a platform for investigation of interesting chemistry and physics with relevance to devices.

It has been fundamentally interesting to characterize the existence of ferroelectricity in ultrathin films^{46,47} and determine the limit on the thickness^{48,49} of an oxide ferroelectric film. Even films with 1 nm thickness were found experimentally to exhibit ferroelectricity.⁴⁶ We point out a recent first-principles prediction⁵⁰ of the emergence of ferroelectricity at a metal–semiconductor transition in 2-D MoS₂ making it the world’s thinnest ferroelectric and a semiconductor. In this case, ferroelectricity is *improper*, arising from trimerization of Mo atoms, and hence does not have a size limit in principle! Based on this, dipoletronic devices have been proposed based on the coupling between the ferroelectric dipoles and free carriers of semiconducting MoS₂. Thus, it appears possible that many new exciting directions of materials research can be opened up essentially from first-principles.

■ CONCLUSIONS

A combination of first-principles DFT and modeling has been very powerful and effective in studies of ferroelectric materials and their structural phase transitions. In addition to precisely pointing out charge transfer as the dominant chemical mechanism of ferroelectricity in perovskite oxides, it has led to prediction of novel ferroelectrics, mapping of the electric field–temperature phase diagrams, and determination of size dependent behavior of nanoscale ferroelectric films and their strain–temperature phase diagrams. The first-principles free energy landscape of a ferroelectric has shed light on the nature of its first-order transition with important role played by polarization fluctuations. Thus, divergence-free inhomogeneous ordering of polarization is expected to be common in the nanoscale ferroelectric structures where the boundary conditions suppress uniform polarization. The contrast between the transition behavior and domain structures of BaTiO₃ and PbTiO₃ has been traced to the disparity in their strain–phonon coupling at the microscopic level. It is highly satisfying that coarse-graining based modeling strategy facilitates access to processes at longer length and time scales while preserving the material specificity of first-principles techniques. Indeed, the multiscale modeling strategy sketched here is expected to work for other classes of smart materials like shape memory alloys, which undergo a nondiffusive structural transition that is central to their memory effect, and has been generalized to multiferroics, which exhibit ferroelectricity as well as magnetic ordering.⁵¹ There are of course many more problems involving relaxor behavior, heterostructures, and sub-gigahertz dynamical properties of ferroelectrics that pose challenges to be overcome by first-principles theoretical analysis.

AUTHOR INFORMATION

Corresponding Author

*E-mail: waghmare@incasr.ac.in.

Author Contributions

The manuscript is based on works completed by the author through collaboration with the researchers acknowledged. The manuscript was written by the author.

Funding

This work was supported by a Department of Atomic Energy-Outstanding Researcher Grant and a J C Bose National Fellowship of the Department of Science and Technology, Government of India.

Notes

The authors declare no competing financial interest.

Biography

Umesh Waghmare received a B. Tech. (with institute silver medal) in Engineering Physics from the IIT, Bombay (1990), and a Ph.D. in Applied Physics from Yale University (1996). He worked as a postdoctoral research associate in the physics department at Harvard University before joining Jawaharlal Nehru Centre for Advanced Scientific Research in 2000, where he is presently a Professor and Chairman in the Theoretical Sciences Unit. His research interests include *ab initio* modeling and simulations of multifunctional materials, mechanical behavior, nanostructures, topological insulators, and materials for energy and environment.

ACKNOWLEDGMENTS

We acknowledge collaborations and useful discussions with T. Nishimatsu, Summayya Kouser, Sharmila Shirodkar, Anil Kumar, Jaita Paul, Joydeep Bhattacharjee, Y. Kawazoe, K. M. Rabe, and D. Vanderbilt.

REFERENCES

- (1) Lines, M. E.; Glass, A. M. *Principles and Applications of Ferroelectrics and Related Materials*; Oxford University Press: New York, 2001.
- (2) Cohen, R. E. Origin of Ferroelectricity in Perovskite Oxides. *Nature* **1992**, *358*, 136–138.
- (3) Rappe, A. M.; Rabe, K. M.; Kaxiras, E.; Joannopoulos, J. D. Optimized Pseudopotentials. *Phys. Rev.* **1990**, *B41*, 1227–1230(R).
- (4) Vanderbilt, D. Soft Self-Consistent Pseudopotentials in a Generalized Eigenvalue Formalism. *Phys. Rev.* **1990**, *B41*, 7892–7895.
- (5) Vanderbilt, D. First-Principles Based Modelling of Ferroelectrics. *Curr. Opin. Solid State Mater. Sci.* **1997**, *2*, 701–705.
- (6) Giannozzi, P.; Baroni, S.; Bonini, N.; Calandra, B.; Car, R.; Cavazzoni, C.; Ceresoli, D.; Chiarotti, G. L.; Cococcioni, M.; Dabo Corso, A.; de Gironcoli, S.; Fabris, S.; Fratesi, G.; Gebauer, R.; Gerstmann, U.; Gougoussis, C.; Kokalj, A.; Lazzeri, M.; Martin-Samos, L.; Marzari, N.; Mauri, F.; Mazzarello, R.; Paolini, S.; Pasquarello, A.; Paulatto, L.; Sbraccia, C.; Scandolo, S.; Sclauzero, G.; Seitonen, A. P.; Smogunov, A.; Umari, P.; Wentzcovitch, R. M. QUANTUM ESPRESSO: A Modular and Open-Source Software Project for Quantum Simulations of Materials. *J. Phys: Condens. Matter* **2009**, *21*, No. 395502.
- (7) Gonze, X.; Amadon, B.; Anglade, P.-M.; Beuken, J.-M.; Bottin, F.; Boulanger, P.; Bruneval, F.; Caliste, D.; Caracas, R.; Côté, M.; Deutsch, T.; Genovese, L.; Ghosez, Ph.; Giantomassi, M.; Goedecker, S.; Hamann, D. R.; Hermet, P.; Jollet, F.; Jomard, G.; Leroux, S.; Mancini, M.; Mazevet, S.; Oliveira, M. J. T.; Onida, G.; Pouillon, Y.; Rangel, T.; Rignanese, G.-M.; Sangalli, D.; Shaltaf, R.; Torrent, M.; Verstraete, M. J.; Zerah, G.; Zwanziger, J. W. ABINIT: First-principles

approach of materials and nanosystem properties. *Comput. Phys. Commun.* **2009**, *180*, 2582–2615.

(8) King-smith; Vanderbilt, D. Theory of polarization of crystalline solids. *Phys. Rev.* **1993**, *B47*, 1651–1654(R).

(9) Marzari, N.; Vanderbilt, D. Maximally Localized Wannier Functions. *Phys. Rev.* **1997**, *B56*, 12847–12865.

(10) Riener, J. W.; Walker, F. J.; Ahn, C.-H. Atomically Engineered Oxide Interfaces. *Science* **2009**, *323*, 1018–1019.

(11) Rabe, K. M., Ahn, C.-H., Triscone, J.-M., Eds. *Physics of Ferroelectrics: A Modern Perspective*; Springer-Verlag: Berlin, Heidelberg, 2007.

(12) Waghmare, U. V. Theory of Ferroelectricity and Size Effects in Thin Films. In *Thin Film Metal-Oxides: Fundamentals and Applications in Electronics and Energy*; Ramanathan, S., Ed.; Springer: New York, 2010; pp 205–233.

(13) Baettig, P.; Schelle, C. F.; LeSar, R.; Waghmare, U. V.; Spaldin, N. A. Theoretical Prediction of New High-Performance Lead-Free Piezoelectrics. *Chem. Mater.* **2005**, *17*, 1376–1380.

(14) Pal, A.; Shirodkar, S. N.; Gohil, S.; Ghosh, S.; Waghmare, U. V.; Ayyub, P. Multiferroic Behavior in Elemental Selenium below 40 K: Effect of Electronic Topology. *Sci. Rep.* **2013**, *3*, No. 2051.

(15) Zhong, W.; King-Smith, R. D.; Vanderbilt, D. Giant LO-TO Splittings in Perovskite Ferroelectrics. *Phys. Rev. Lett.* **1994**, *72*, 3618–3621.

(16) Waghmare, U. V.; Spaldin, N. A.; Kandpal, H. C.; Seshadri, R. First-Principles Indicators of Metallicity and Cation Off-centricity in the IV-VI Rocksalt Chalcogenides of Divalent Ge, Sn, and Pb. *Phys. Rev.* **2003**, *B67* (12), No. 125111.

(17) Bhattacharjee, J.; Waghmare, U. V. Wannier Orbital Overlap Population (WOOP), Wannier Orbital Position Population (WOPP) and the Origin of Anomalous Dynamical Charges. *Phys. Chem. Chem. Phys.* **2010**, *12* (7), 1564–1570.

(18) Posternak, M.; Resta, R.; Baldereschi, A. Role of Covalent Bonding in the Polarization of Perovskite Oxides: The Case of KNbO_3 . *Phys. Rev.* **1994**, *B50*, 8911–8914.

(19) Ghosez, Ph.; Michenaud, J.-P.; Gonze, X. Dynamical Atomic Charges: The Case of ABO_3 Compounds. *Phys. Rev.* **1998**, *B58*, 6224–6240.

(20) Bhattacharjee, J.; Waghmare, U. V. Localized Orbital Description of Electronic Structures of Extended Periodic Metals, Insulators, And Confined Systems: Density Functional Theory Calculations. *Phys. Rev.* **2006**, *B73*, 121102.

(21) Safari, A.; Bousquet, E.; Katcho, K.; Ghosez, Ph. First-Principles Study of Structural and Vibrational Properties of SrZrO_3 . *Phys. Rev.* **2012**, *B85*, No. 064112.

(22) Bennett, J. W.; Garrity, K. F.; Rabe, K. M.; Vanderbilt, D. Hexagonal ABC Semiconductors as Ferroelectrics. *Phys. Rev. Lett.* **2012**, *109*, No. 167602.

(23) Ghosez, P.; Cockayne, E.; Waghmare, U. V.; Rabe, K. M. Lattice Dynamics of BaTiO_3 , PbTiO_3 , and PbZrO_3 : A Comparative First-Principles Study. *Phys. Rev.* **1999**, *B60* (2), 836–843.

(24) Rabe, K. M.; Waghmare, U. V. Localized Basis for Effective Lattice Hamiltonians- Lattice Wannier functions. *Phys. Rev.* **1995**, *B52*, 13236–13246.

(25) Zhong, W.; Vanderbilt, D. Effect of Quantum Fluctuations on Structural Phase Transitions in SrTiO_3 and BaTiO_3 . *Phys. Rev.* **1996**, *B53*, 5047–5050.

(26) Zhong, W.; Vanderbilt, D.; Rabe, K. M. Phase Transitions in BaTiO_3 from First Principles. *Phys. Rev. Lett.* **1994**, *73*, 1861–1864.

(27) Waghmare, U. V.; Rabe, K. M. Ab Initio Statistical Mechanics of the Ferroelectric Phase Transition in PbTiO_3 . *Phys. Rev.* **1997**, *B55*, 6161–6173.

(28) Waghmare, U. V.; Cockayne, E. J.; Burton, B. P. Ferroelectric Phase Transitions in Nano-scale Chemically Ordered $\text{PbSc}_{0.5}\text{Nb}_{0.5}\text{O}_3$ Using a First-Principles Model Hamiltonian. *Ferroelectrics* **2003**, *291*, 187–196.

(29) Nishimatsu, T. FERAM code. <http://loto.sf.net/feram/>.

(30) Nishimatsu, T.; Waghmare, U. V.; Kawazoe, Y.; Vanderbilt, D. Fast Molecular-Dynamics Simulation for Ferroelectric Thin-Film

Capacitors Using a First-Principles Effective Hamiltonian. *Phys. Rev.* **2008**, *B78*, No. 104104.

(31) Paul, J.; Nishimatsu, T.; Kawazoe, Y.; Waghmare, U. V. Ferroelectric Phase Transitions in Ultrathin Films of BaTiO₃. *Phys. Rev. Lett.* **2007**, *99*, No. 077601.

(32) Nishimatsu, T.; Iwamoto, M.; Kawazoe, Y.; Waghmare, U. V. First-Principles Accurate Total Energy Surfaces for Polar Structural Distortions of BaTiO₃, PbTiO₃, and SrTiO₃: Consequences for Structural Transition Temperatures. *Phys. Rev.* **2010**, *B82* (13), No. 134106.

(33) Paul, J.; Nishimatsu, T.; Kawazoe, Y.; Waghmare, U. V. Polarization Rotation, Switching, And Electric-Field-Temperature Phase Diagrams of Ferroelectric BaTiO₃: A Molecular Dynamics Study. *Phys. Rev.* **2009**, *B80*, No. 024107.

(34) Fu, H.; Cohen, R. E. Polarization Rotation Mechanism for Ultrahigh Electromechanical Response in Single-Crystal Piezoelectrics. *Nature* **2000**, *403*, 281–283.

(35) Paul, J.; Nishimatsu, T.; Kawazoe, Y.; Waghmare, U. V. Polarization Switching in Epitaxial Films of BaTiO₃: A Molecular Dynamics Study. *Appl. Phys. Lett.* **2008**, *93*, No. 242905.

(36) Shin, Y.-H.; Grinberg, I.; Chen, I.-W.; Rappe, A. M. Nucleation and Growth Mechanism of Ferroelectric Domain-Wall Motion. *Nature* **2007**, *449*, 881–884.

(37) Aguado-Puente, P.; Junquera, J. Ferromagnetic-like Closure Domains in Ferroelectric Ultrathin Films: First-Principles Simulations. *Phys. Rev. Lett.* **2008**, *100*, No. 177601.

(38) Prosandeev, S.; Bellaiche, L. Asymmetric Screening of the Depolarizing Field in a Ferroelectric Thin Film. *Phys. Rev.* **2007**, *B75*, No. 172109.

(39) Kouser, S.; Nishimatsu, T.; Waghmare, U. V. Ferroelectric Domains and Diffuse Transitions in Ultrathin Films of PbTiO₃: Effects of Strain and Electrodes. *Phys. Rev.* **2013**, *B88*, No. 064102.

(40) Kumar, A.; Rabe, K. M.; Waghmare, U. V. Domain Formation and Dielectric Response in PbTiO₃: A First-Principles Free Energy Landscape Analysis. *Phys. Rev.* **2013**, *B87*, No. 024107.

(41) Kumar, A.; Waghmare, U. V. First-Principles Free Energies and Ginzburg-Landau Theory of Domains and Ferroelectric Phase Transitions in BaTiO₃. *Phys. Rev.* **2010**, *B82*, No. 054117.

(42) Nishimatsu, T.; Aoyagi, K.; Kiguchi, T.; Konno, T. J.; Kawazoe, Y.; Funakubo, H.; Kumar, A.; Waghmare, U. V. Molecular Dynamics Simulation of 90 degrees Ferroelectric Domains in PbTiO₃. *J. Phys. Soc. Jpn.* **2012**, *81*, No. 124702.

(43) Burton, B. P.; Cockayne, E.; Tinte, S.; Waghmare, U. V. First-Principles-Based Simulations of Relaxor Ferroelectrics. *Phase Transitions* **2006**, *79*, 91–121.

(44) Burton, B. P.; Cockayne, E.; Waghmare, U. V. Correlations between Nanoscale Chemical and Polar Order in Relaxor Ferroelectrics and the Lengthscale for Polar Nanoregions. *Phys. Rev.* **2005**, *B72*, No. 064113.

(45) Kumar, N.; Pan, J.; Aysha, N.; Waghmare, U. V.; Sundaresan, A.; Rao, C. N. R. Effect of Co-substitution of Nitrogen and Fluorine in BaTiO₃ on Ferroelectricity and Other Properties. *J. Phys.: Condens. Matter* **2013**, *25*, No. 345901.

(46) Fong, D. D.; Stephenson, G. B.; Streiffer, S. K.; Eastman, J. A.; Auciello, O.; Fuoss, P. H.; Thompson, C. Ferroelectricity in Ultrathin Perovskite Films. *Science* **2004**, *304*, 1650–1653.

(47) Choi, K. J.; Biegalski, M.; Li, Y. L.; Sharan, A.; Schubert, J.; Uecker, R.; Reiche, P.; Chen, Y. B.; Pan, X. Q.; Gopalan, V.; Chen, L. Q.; Schlom, D. G.; Eom, C. B. Enhancement of Ferroelectricity in Strained BaTiO₃ Thin Films. *Science* **2004**, *306*, 1005–1009.

(48) Junquera, J.; Ghosez, P. Critical Thickness for Ferroelectricity in Perovskite Ultrathin Films. *Nature* **2003**, *422*, 506–509.

(49) Spaldin, N. A. Fundamental Size Limits on Ferroelectricity. *Science* **2004**, *304*, 1606–1607.

(50) Shirodkar, S. N.; Waghmare, U. V. Emergence of Ferroelectricity at a Metal-Semiconductor Transition in a 1T Monolayer of MoS₂. *Phys. Rev. Lett.* **2014**, *112*, No. 157601.

(51) Kornev, I. A.; Lisenkov, S.; Haumont, R.; Dkhil, B.; Bellaiche, L. Finite-Temperature Properties of Multiferroic BiFeO₃. *Phys. Rev. Lett.* **2007**, *99*, No. 227602.